JOURNAL OF MATERIALS SCIENCE **40** (2005) 3467–3474

Effect of O_2 partial pressure and thickness on the gasochromic properties of sputtered V_2O_5 films

H. SHANAK[1], H. SCHMITT[1,*], J. NOWOCZIN[1], K.-H. EHSES[2]
Universität des Saarlandes, [1]Technische Physik and [2]Experimentalphysik, D- 66123 Saarbruecken, Germany
E-mail: heschmitt@mx.uni-saarland.de

V_2O_5 thin films were deposited by reactive DC-diode sputtering technique in a mixed atmosphere of O_2/Ar gas at room temperature from a high purity target of 99.99% vanadium. For the investigation, the thickness of the films and the O_2/Ar ratio during the sputtering process were the parameters. The sputtering rate of the V_2O_5 films dramatically decreases with increasing the O_2/Ar ratio. By X-ray diffraction it was found that films sputtered with 1% O_2/Ar ratio grow preferentially in two orientations: the 200 and the 001 orientation. The increase of the O_2/Ar ratio enhances the growth preferentially in the *c*-axis (001) and strongly decreases the growth in the *a*-axis (200) direction. The scanning electron microscope pictures confirm these results. In the visible region the optical transmittance is increased with increasing the O_2/Ar ratio in the sputter gas. Additionally, the optical band gap is slightly larger for the films sputtered with an O_2/Ar ratio higher than 5%. Beyond a thickness of about 220 nm and an O_2/Ar ratio of 10% the electrical sheet resistance of the films increases dramatically. During the insertion/extraction of hydrogen ions, the change in the optical transmission was investigated. The gasochromism of the V_2O_5 films was explained by use of the Infra Red (IR) measurements during the insertion/extraction of hydrogen ions.

1. Introduction

Among the transition metal oxides the vanadium-oxygen system is remarkable and even in a certain sense, unique. The point is that the vanadium forms more than ten distinct oxide phases with different electronic properties, ranging from metallic to insulating: VO; V_2O_3; V_nO_{2n-1} series with n from 3 to 8; VO_2; V_2O_5 [1]. The vanadium pentaoxide (V_2O_5) and the dioxide (VO_2) thin films were the most investigated of the different vanadium oxides because of their potential for application in different scientific and technological areas [2]. It can be used as gas sensor, as cathode for solid-state batteries, as window for solar cells, as electronic and optical switches, and as ion storage for an electrochromic device [3]. Vanadium oxide is a promising material in energy storage systems and has a high ionic storage capacity due to its layered structure [4]. The possibility to prepare the vanadium oxide at room temperature by a vacuum method such as sputtering is of a great advantage for on-chip applications [5]. To prepare thin films of vanadium oxide, in addition to the sputtering technique by several other authors, other methods such as vacuum evaporation [6], chemical vapor deposition [7], sol–gel technique [8] and pulsed laser deposition [9, 10] have been used. It has been recognized that V_2O_5 can be colored by electro-, photo-, and thermochromic processes [11]. Most research has been focused on electrochromic coloration of this material. The process is usually described in terms of the double injection/extraction model of ions and electrons (Equation 1):

$$V_2O_5 + xA^+ + xe^- = A_xV_2O_5 \qquad (1)$$

where A = H or Li. During the coloration in these films V^{5+} undergoes a reduction to V^{4+} [11, 12]. Different experimental and theoretical investigations of the electrochromism of other materials such as WO_3 and the interpretation of its coloration with H^+ and D^+ cations were recently published [13–16].

Electrochromic materials are usually classified into cathodically or anodically coloring materials depending on the direction of the change of coloration due to ion intercalation. The optical transmittance of the cathodic coloration materials decrease with the intercalation of ions and electrons. The behavior of the transmittance is opposite in the case of the anodic coloration materials. But vanadium pentoxide shows a more complicated behavior of coloration. It shows as well cathodically as anodically coloration. This behavior has been interpreted in terms of the band structure [12, 17]. Besides this, there is a lack of information about the thickness dependence and preferentially the influence of the gas composition during the sputtering process.

*Author to whom all correspondence should be addressed.

In this work V_2O_5 films were gasochromicaly colored/bleached with the spill-over method by exposing them to hydrogen and oxygen gas respectively. The influence of the film thickness and the O_2/Ar ratio during the sputtering process on the coloration/ bleaching was investigated. In the case, when the thickness was changed, the O_2/Ar ratio was kept constant and vice versa. For the application of V_2O_5 films in gasochromic devices, as ion storages in electrochromic devices and as high quality hydrogen sensors a reproducible and optimized production process is essential. For this reason a precise controlling of the production parameters as well as its optimization is necessary.

2. Experimental

V_2O_5 thin films were deposited by reactive DC-diode sputtering technique in a mixed atmosphere of O_2/Ar gas at room temperature from a high purity target of 99.99% vanadium. As substrates glasses which were ultrasonically cleaned in propanol and Si wafer (for IR- and X-ray diffraction measurements) were used. The target-substrate distance was kept constant to be 35 mm. Before the gases were introduced, the vacuum in the sputtering chamber had a base pressure of $\sim 1.5 \times 10^{-6}$ mbar. The total sputtering pressure was kept constant to be 0.1 mbar. During the sputtering process, the reactive gas (O_2) and the argon were continuously supplied, the flow and ratio of both gases were automatically controlled and regulated by use of a mass spectrometer. The digital signals of the charactaristical mass peaks are given via digital analog converters (DAC) to regulating systems (PID). The PID systems drive two gas valves to control and regulate the partial pressure of O_2 and Ar in the sputtering chamber. The total pressure - i.e. the sum of the partial pressures of Ar and O_2- in the chamber is controlled by a gas type independent membrane system (MKS Baratron). The sputtering voltage was 2 kV resulting in a sputtering power density of 1 W/cm^2. The thickness of the films was measured at cross sections by use of a scanning electronmicroscope (SEM) and with the Tolansky method. The Tolansky method uses optical interference fringes and their shift at a step between the film and the non covered substrate. The sputtering rate was calculated as the quotient of the film thickness and the sputtering time. The sputtering rate dramatically decreases from 0.9 nm/min when the O_2/Ar ratio is 1% to 0.40 nm/min when the O_2/Ar ratio is larger than 10%.

For the thin films which were colored/bleached by the insertion/extraction of H^+ ions by the spill-over method, a very small amount of Pt-catalyst (2.65 μg/cm^2) was sputtered onto the top of the V_2O_5 films [18]. The coloration/bleaching processes were carried out in a continuous flow of hydrogen and oxygen gas respectively. To remove any impurities which may exist at the surface of the electrochromic films or in the surrounding atmosphere (e.g. humidity), the V_2O_5/Pt films are exposed to Ar gas at the starting point and as well between the switching from the coloration process with hydrogen to the bleaching process with oxygen in order to avoid any external reactions between oxygen and hydrogen [18, 19]. The purity of O_2 used is 99.996%, of H_2 is 99.9% and of Ar is 99,998%. The coloration was performed at atmospheric pressure and at room temperature. During the coloration/bleaching process at a wavelength of 633 nm the optical transmittance as a function of time was measured. For this purpose a He-Ne laser of 1 mW power and silicon photodiodes as sensors were used [18, 19]. To erase variations of the intensity of the laser light, a second beam splitted from the same laser was used as a reference. A schematic set up of the experiment is shown in Fig 1.

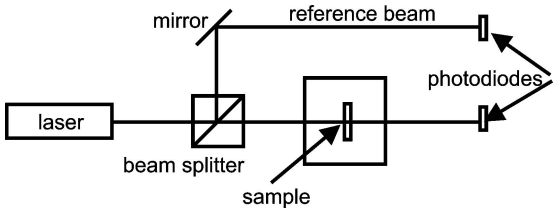

Figure 1 Set up for the investigation of the transmission behavior during coloration and bleaching.

X-ray diffraction (XRD) measurements were carried out on the films with Cu Kα radiation by use of the Scherrer geometry. The measurements were performed with a resolution of 0.02 degree, the measuring time per step was 20 s. The film morphology was examined with a scanning electron microscope (SEM). The optical transmittance spectra of the films at normal incidence were measured with a double beam recording UV-Vis-NIR spectrophotometer (Hitachi, Model U–3501). A Perkin Elmer System 2000 spectrometer was used for ex-situ FT-IR spectroscopic measurements. For the IR-measurements, as a substrate for the films, 100 silicon was used. To determine the base line the identical substrate material was measured and subtracted. The sheet resistance $R_\square$ of the V_2O_5/Pt system was measured with a DMM (KEITHLEY 2000) by use of the four point method. The measuring current was 0.1 mA or lower.

3. Result and discussion

3.1. Structural analysis and morphology

The XRD patterns of the as-deposited films sputtered with different O_2/Ar ratios and constant thickness ($\approx$700 nm) onto glass and silicon substrates were shown in Fig. 2a and b respectively. The peaks were indexed assuming an orthorhombic structure of V_2O_5 [17]. It was found that the grains of films sputtered with low O_2/Ar ratio (1%) grow preferentially in two orientations: the 200 and the 001 orientation. The increasing of the O_2/Ar ratio enhances the growth preferentially in the *c*-axis (001) direction. The peaks of the (200) orientation decrease with increasing O_2/Ar ratio and become very small for films produced at high O_2/Ar ratios (20%). Additionally, a small peak at 26.37° (110) appears for the films sputtered with 10 and 20% O_2/Ar ratios. The same tendency can be seen for the films deposited as well onto glass as onto silicon substrates.

Films deposited at different thickness and at constant O_2/Ar ratio of 1% onto glass and Si are presented

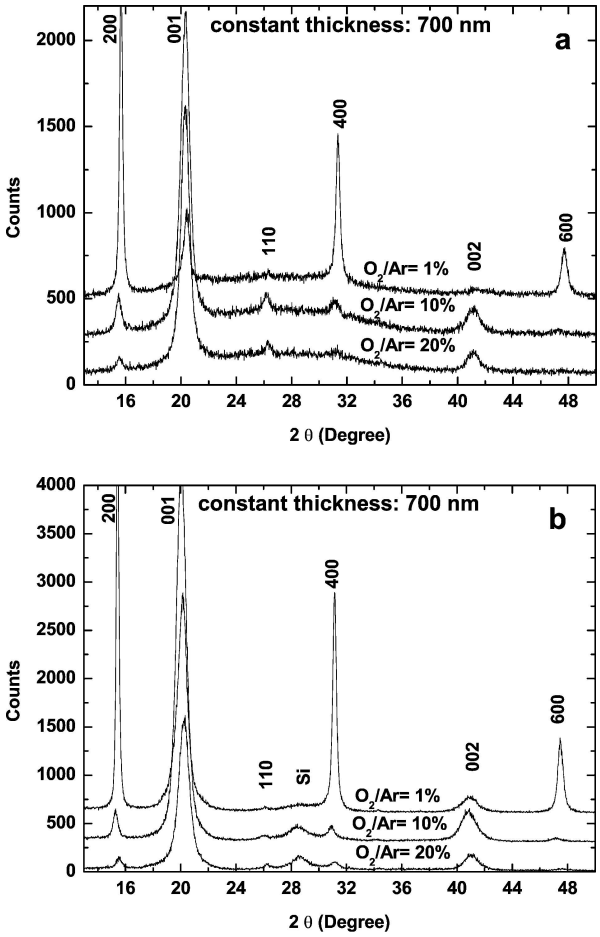

Figure 2 X-ray diffractogram of as-deposited V_2O_5 films as a function of O_2/Ar ratio; (a) onto glass, (b) onto Si.

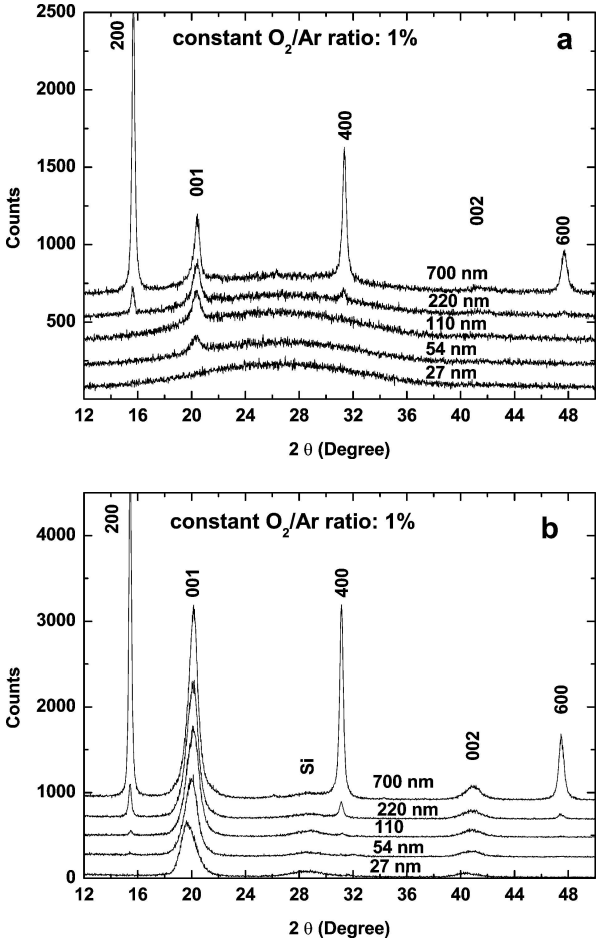

Figure 3 X-ray diffractogram of as-deposited V_2O_5 films as a function of thickness; (a) onto glass, (b) onto Si.

in Fig. 3a and b respectively. The growth of the grains starts initially in the *c*-axis (001) direction until a specific value of about 220 nm is reached as it can be seen from Fig. 3a and b. Beyond a thickness of ~220 nm, the growth is clear in the *a*-axis (200) as well as in the *c*-axis (001). To determine the thickness at which the growth starts in the *a*-axis (200) direction. The intensity of the peaks for all reflections in Fig. 3a and b were plotted against the thickness of the films as it is shown in Fig. 4. The extrapolation of the lines of the 200, 400 and 600 peaks which represent the growth in the a-direction, show that the growth in this direction starts originally with the thickness of about 185 nm.

From the XRD patterns, the grain size of the grains in both orientations 001 and 200 was determined for the different samples by use of a Williamson-Hall-Plot [20]. It was found that for the samples sputtered at low O_2/Ar ratio (1%), the grain size of the grains in the a-direction (200) was larger than that one in the c-direction (001). One can see that if the ratio of O_2/Ar increases to 10 and 20% the grain size in the a-direction decreases severely, but in the c-direction the change is not large. In this case the difference between the grain size in the a- and c-direction is very small for the samples sputtered onto glass, and is a little larger for the samples sputtered onto silicon, as it is shown in Fig. 5. In all cases the grain size remains in the nanoscale region.

SEM pictures confirm the behavior of the grain size with the change in the O_2/Ar ratio. In Fig. 6a and b, the

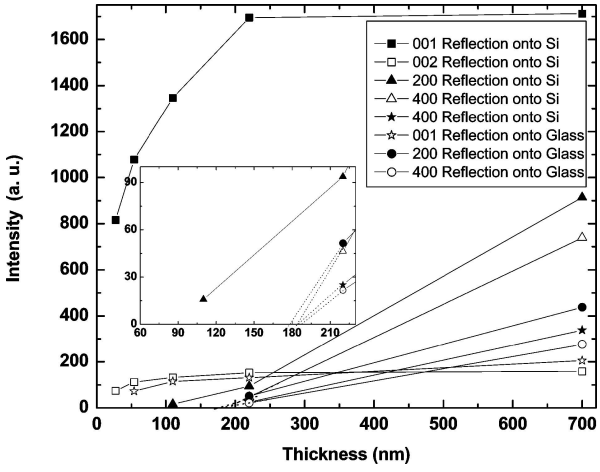

Figure 4 Intensity of the X-ray diffraction peaks as a function of thickness with const O_2/Ar ratio (1%) onto glass and Si.

surface of the sample sputtered with low O_2/Ar ratio (1%) onto glass and Si appears as needles. It is expected that the length of these needles express the growth in one direction (200), and the height (the diameter of the needles) express the growth in the (001) direction. In case of high O_2/Ar ratio (20%), the length become slightly larger than the diameter, therefore the grain size in the a-direction become slightly larger than in c-direction (Fig. 7a and b).

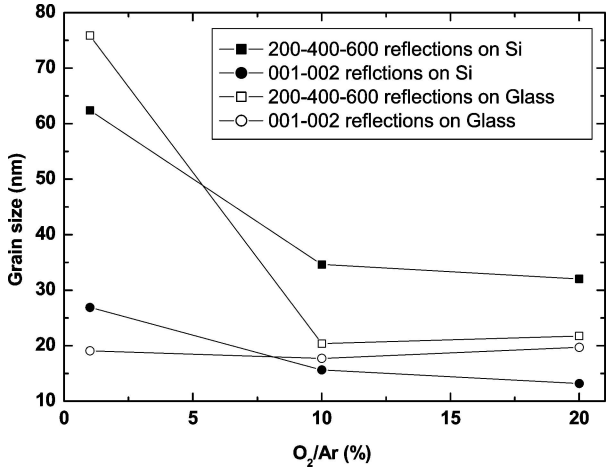

Figure 5 The grain size as a function of O_2/Ar ratio, calculated from (*h*, *k*, *l* indices) by a Williamson-Hall-Plot (film thickness: 700 nm).

3.2. UV/Vis

Fig. 8a shows the transmission of the as-deposited films sputtered with different thickness and at constant O_2/Ar ratio of 1%. The transmission spectrum can be divided into three main regions. In the first one, between 300–490 nm the transmission decreases with increasing the thickness. In the third region for $\lambda > 800$ nm it decreases again with the thickness. In the second region between $\lambda = 490$–800 nm however, the behavior of the transmission as a function of the sample thickness is not monotonic. The as-deposited films sputtered with constant thickness (≈80 nm) but with different O_2/Ar ratios (1–30)% show nearly the same behavior in the wave length ranges lower than 490 nm and higher than 800 nm as in the case of constant O_2/Ar ratio and different thickness, but between 490 and 800 nm the transmission increases with increasing O_2/Ar as it is shown in Fig. 8b.

After the second cycle of the intercalation/deintercalation processes, the transmission spectrum as a function of wavelength was measured for the same samples again, and it was found that the transmission was clearly increased in the region of wavelength lower than 490 nm, and decreased in the range of wavelength $\lambda = 490$–800 nm. This behavior was found for both series: the films with different thickness and constant O_2/Ar ratio, and for the films with different O_2/Ar ratio and constant thickness.

In order to determine the optical energy gap E_g, $(\alpha h\nu)^n$ was plotted as a function of $h\nu$. The best fit for our data was found with $n = 2$, which indicates an allowed direct transition. The energy gap is nearly constant with a slight increase with increasing O_2/Ar ratio

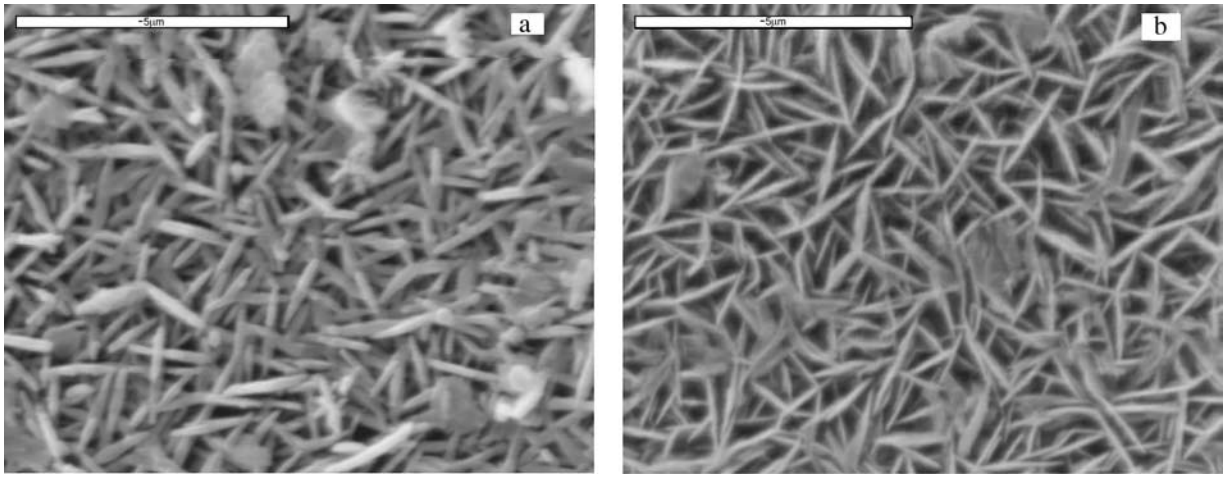

Figure 6 SEM pictures of V_2O_5 films of a thickness of 700 nm, sputtered with O_2/Ar = 1% onto glass (a) and onto Si (b).

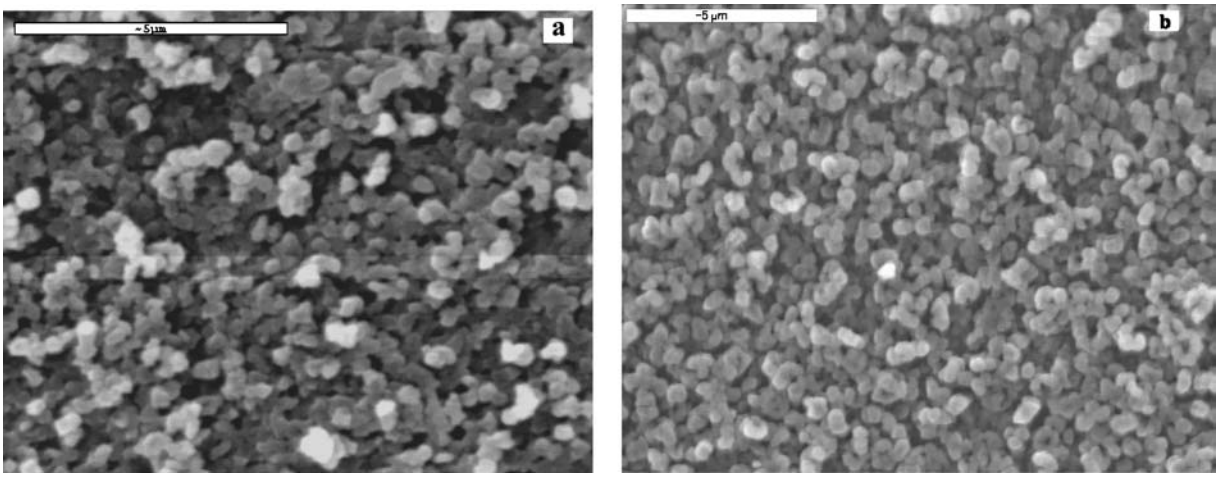

Figure 7 SEM pictures of V_2O_5 films of a thickness of 700 nm, sputtered with O_2/Ar = 20% onto glass (a) and onto Si (b).

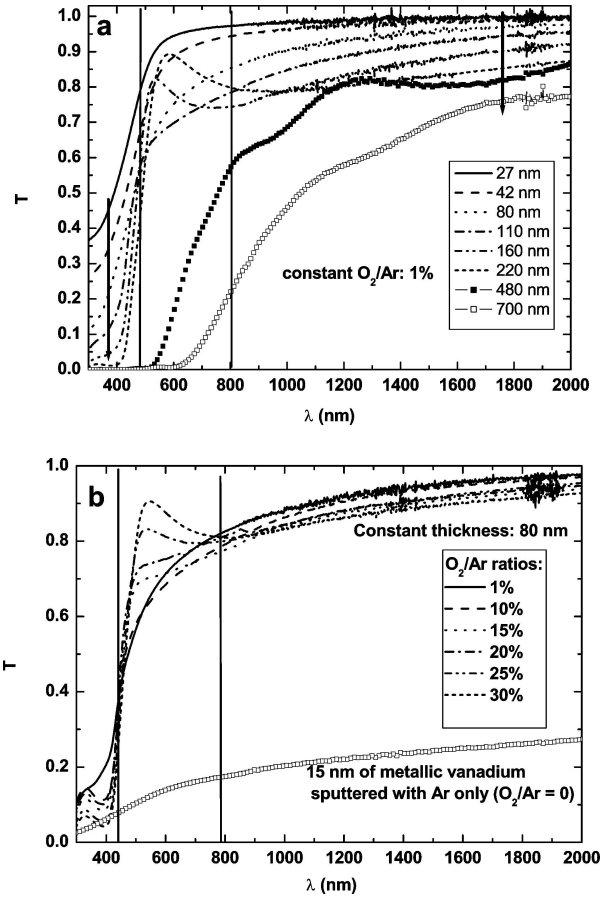

Figure 8 Optical transmittance versus wavelength of the as-deposited V_2O_5 films as a function of thickness (a) and as a function of O_2/Ar ratio (b). For comparison, a spectrum of metallic vanadium film is added. (The lines mark the different wavelength regions described in the text).

for the as-deposited films with constant thickness. It is also constant for the films with a thickness less than 80 nm and larger than 220 nm. A slight increase of the E_g for the films with a thickness between 80 and 220 nm is observed as it is presented in Fig. 9. An enlargement of the E_g was measured after the second cycle of intercalation/deintercalation, where it was increased from $E_g \approx 2.6$ eV for the virgin films to $E_g \approx 3.6$ eV for the deintercalated films after the second cycle. The deintercalated film with a thickness of 330 nm has a smaller E_g than the thinner deintercalated ones. The assumption is that, because of the large thickness the H^+ ions does not diffuse until the other side of the film during the intercalation/deintercalation process.

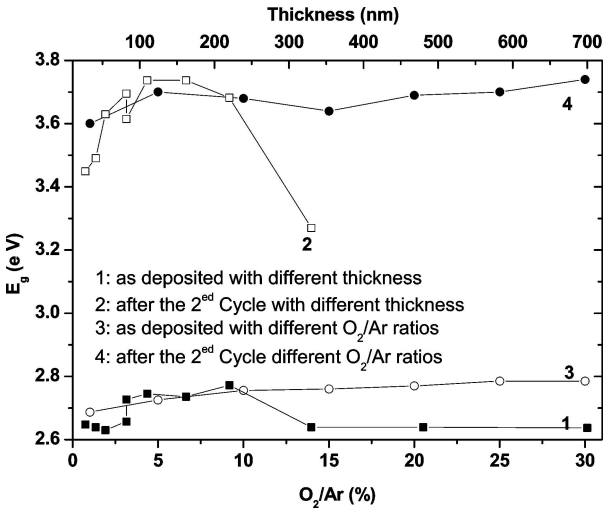

Figure 9 Optical energy gap E_g as a function of the O_2/Ar ratio (lower scale) and of the thickness (upper scale) for the as-deposited films (curves 1 and 3) and after the second cycle of coloration (curves 2 and 4).

3.3. IR-measurements

Fig. 10a shows the IR spectrum of the V_2O_5 films sputtered with different thickness at constant O_2/Ar ratio (1%). The spectrum is dominated by V=O_A (vanadyl) stretching at 1038 cm^{-1} and V—O_B—V stretching at 790 cm^{-1}, bridging the corners of the adjacent VO_5 pyramids. A group of bands below 518 cm^{-1} corresponds to the stretching of oxygens bonded to the three surrounding V-atoms of neighboring edge-shared pyramids ν(3V—O_C) and bridging δ(V—O_B—V) deformations [21]. In the case of very thin films the absorption bands are weak. They become stronger and sharper with increasing the thickness of the films. For wave numbers higher than 2000 cm^{-1} the transmittance of the films is no monotonic function of the film thickness. The curve of the thickest film is located in between the values of the other two thinner films. Interference resulted from the thicker film may be the reason. In Fig. 10b the IR

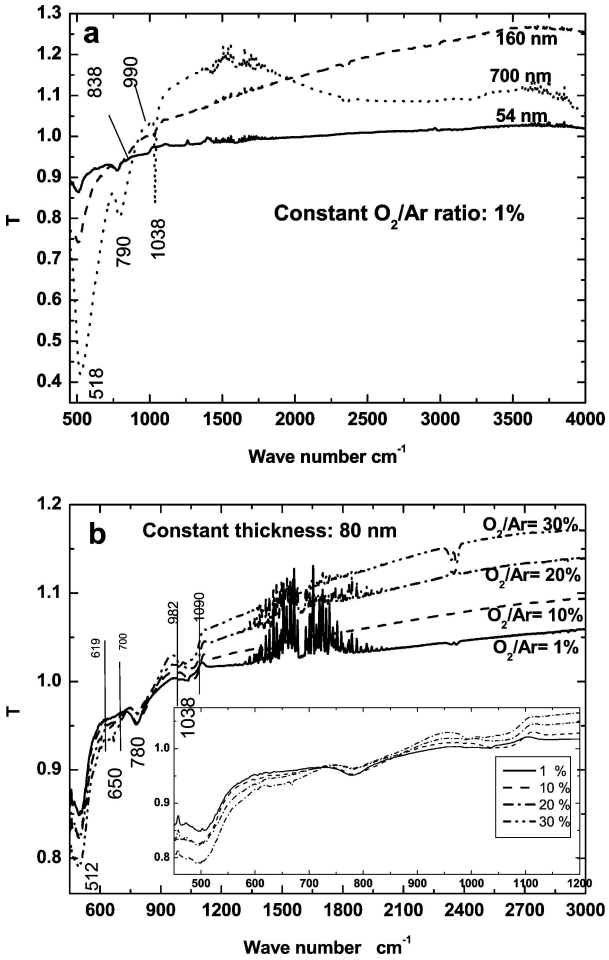

Figure 10 IR spectra of the as-deposited V_2O_5 films as a function of the wavenumber for films with different thickness (a) and different O_2/Ar ratio (b).

spectrum of the thin films of a thickness of ≈80 nm sputtered with different O_2/Ar ratios are shown. The spectra of all samples are dominated by the V—O_B—V stretching at 780 cm^{-1} and a group of bands below 512 cm^{-1}. In case of low O_2/Ar ratio (1%), the V=O_A (vanadyl) stretching at 1038 is not clear but appears as a knee between 1090–990 cm^{-1} and it becomes clear with increasing the O_2/Ar ratio and also a band developed at 650 cm^{-1} for the films sputtered with higher O_2/Ar ratio (≥20%). The prominent band ν(3V—O) at 512 cm^{-1} becomes stronger with increasing the O_2/Ar ratio. Other films with a large thickness of about 700 nm and a high O_2/Ar ratio (20%), show in addition to the three main dominant bands at 1037, 796 and 520 cm^{-1}, a band at 647 cm^{-1} and a shift of the bands to lower wave numbers in comparison with the film sputtered with low O_2/Ar ratio (1%). After the coloration/bleaching processes were completed, the color of the thin films has changed from yellow to gray. This change was irreversible. Therefore we expected that there is a difference between the structure of the virgin V_2O_5 films and the films when the intercalation/deintercalation process has happened.

As shown in Fig. 11a, the IR spectra of the as- deposited and the deintercalated films reveal that there is a shift for the group bands below 513 cm^{-1} and the stretching at 782 cm^{-1} toward higher wave numbers. Both of them become weaker in comparison with the virgin film. Additionally, H-intercalation leads to widening of the bands after the shift to higher wave numbers [21]. Similar shifting was found by other authors and it was explained with the lattice stiffening [22]. In addition to the strengthening of the V=O_A band at 1063,typical bands above 3200 cm^{-1} resulted from the formation of H_2O in $V_2O_5 \cdot nH_2O$ [21, 23]. Simultaneous IR measurements were done during the intercalation/ deintercalation of the films. Fig. 11b shows these changes in the IR spectrum during the intercalation of the H ions into the V_2O_5 films for the first cycle.

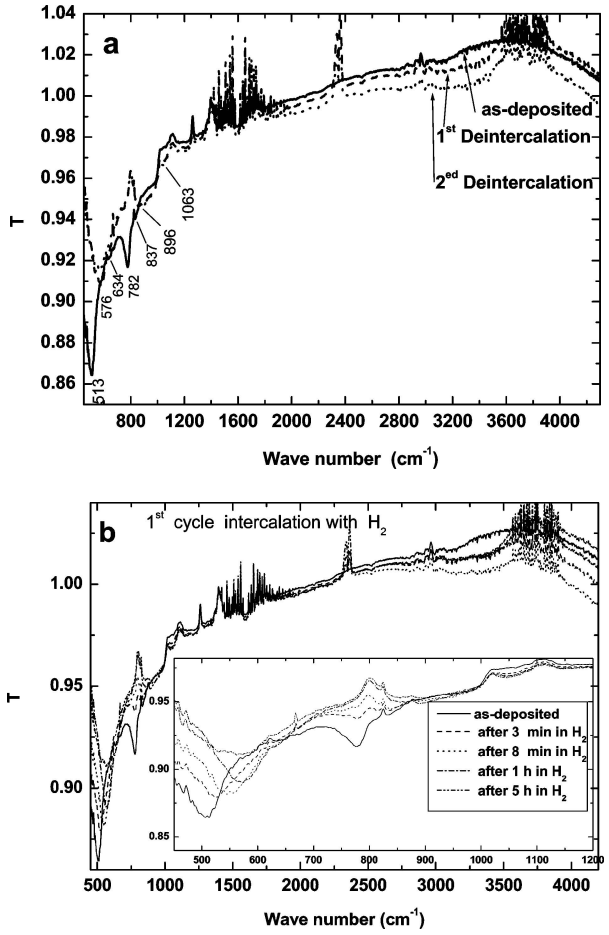

Figure 11 IR spectra of as-deposited and deintercalated film (a), and during intercalation (b), (the thickness of the film is 55 nm, and the O_2/Ar ratio is 1%).

3.4. Intercalation/deintercalation

The change in the normalized transmission of the films with different thickness due to intercalation/deintercalation of the H^+ ions was investigated for the first cycle. The films with a small thickness show a complicated cathodic and anodic electrochromic behavior. The thicker ones show only cathodic behavior. It is known that the vanadium pentoxide, presents a complicated coloration behavior [12, 17]. At the beginning of the intercalation process (low intercalant concentration), it behaves as cathodically coloring material. The transmittance decreases with the intercalation of the hydrogen ions. for some wavelengths region in the visible and until a certain intercalation level; starting from this point of intercalation level, the reverse behavior is observed. It becomes anodic. This means that the transmittance increase with the intercalation of the hydrogen ions. A similar behavior was found also in the IR transmittance during the intercalation at a wave number higher than 2000 cm^{-1}. Such a complicated coloration behavior for the V_2O_5 films was known and explained in terms of the band structure according to other authors [12, 17]. It was found that the behavior of double coloration (cathodic and anodic) in the first cycle was irreversible and all samples have a stable anodic behavior in the second cycle (Fig. 12a) and in all the further following ones. Now the transmission increases with the intercalation of the H^+ ions and decreases with the deintercalation. For the samples sputtered with different O_2/Ar ratio and constant thickness, the anodic behavior improved with increasing the O_2/Ar ratio. Additionally, the samples become more stable anodically after the first intercalation/ deintercalation as shown in Fig. 12b.

3.5. Electrical properties

The film thickness and the O_2/Ar ratio in the sputtering chamber significantly influence the optical properties as it is shown in Section 3.2. The reason for the change in the optical properties by the intercalation of hydrogen is the modification of the energy band structure of the material. Therefore, the film thickness and the O_2/Ar ratio in the sputter gas must influence the electrical properties of the films too. As it is shown in Fig. 13, It was found that the sheet resistance $R_\square$ of the as deposited films sputtered with constant O_2/Ar ratio (1%) jump from a range of a few k Ω to few M Ω beyond a thickness of ∼220 nm. For the samples sputtered with

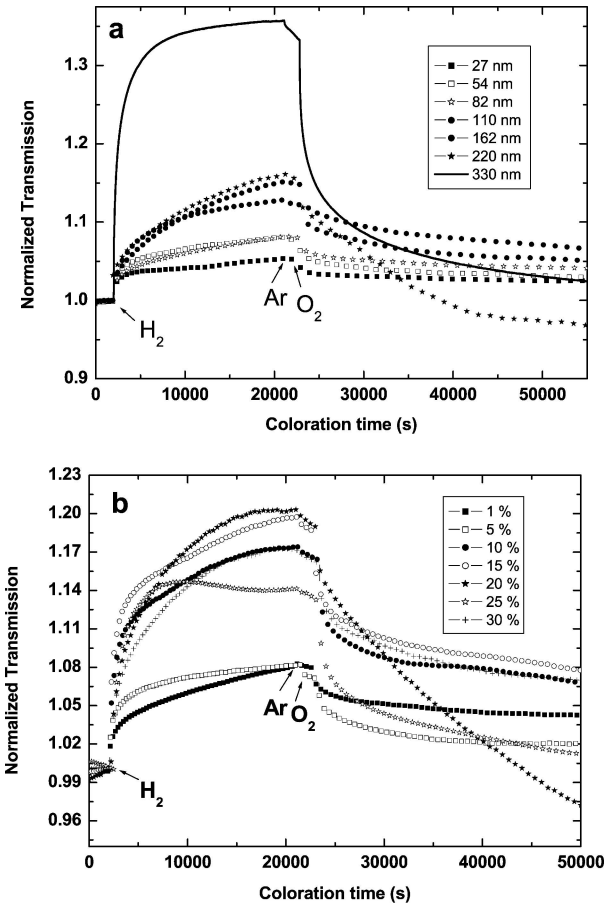

Figure 12 The normalized transmission as a function of the coloration/bleaching time for the second cycle of the V_2O_5 films; (a) with different thickness, (b) with different O_2/Ar ratio.

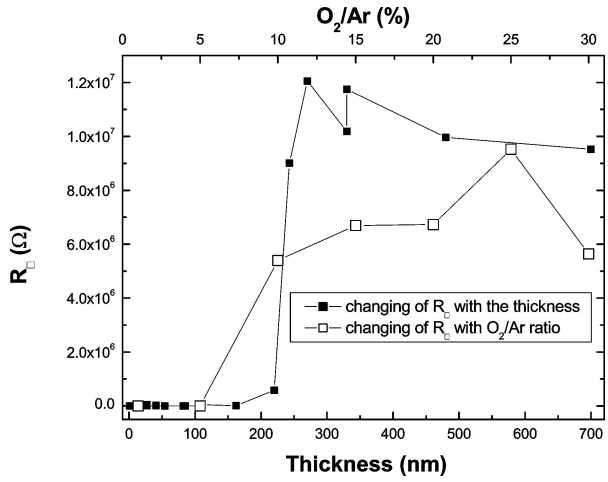

Figure 13 The change in the sheet resistance as a function of thickness (with O_2/Ar = 1%, lower scale) and O_2/Ar ratio (with thickness = 80 nm, upper scale).

constant thickness (80 nm) and different O_2/Ar ratios, $R_\square$ jumps to the higher range when the O_2/Ar ratio is higher than 5%. The reason of this change in $R_\square$ is not quite clear, but it may be related to the change in the microstructure because the XRD measurements show that at this thickness the film grow preferentially in the *a*-axis in addition to the *c*-axis direction. Other authors refers this thickness to be a critical thickness for the properties of V_2O_5 films [24, 12].

4. Conclusions

It was shown that changing the O_2/Ar ratio in the sputtering gas and the thickness of the films have a clear effect on the optical, electrical and structural properties of the V_2O_5 films.

The best V_2O_5 films for gasochromic devices can be received by optimization of the thickness and the O_2/Ar ratio in the sputtering gas. The results are identical for the choose of the films as an ion storage for electrochromic devices. The results show that the preferable V_2O_5 films to be used in gasochromic devices or as ion storages in the electrochromic devices should be sputtered with high O_2/Ar ratio ($\geq$20%) and in a thickness range of 80–100 nm.

The complicated cathodic and anodic coloration of the V_2O_5 films disappears after the first cycle, and the coloration continues as a reversible anodic coloration.

The jumping in $R_\square$ from the range of a few k Ω to the range of some M Ω with increasing both the O_2/Ar ratio and the thickness of the films is may be due to the microstructure change in the films.

Acknowledgements

H. Shanak gratefully acknowledges the financial support from Deutscher Akademischer Austauschdienst (DAAD), Bonn, Germany. The authors thank D. Wallacher for the help by the IR measurements.

References

1. A. PERGAMENT, E. KAZAKOVA and G. STEFANOVICH, *J. Phys. D: Appl. Phys.* **35** (2002) 2187.
2. D. THANH, P. LONG, V. BICH and N. DINH, *Commun. Phys.* **8** (1998) 152.
3. G. FANG, Z. LIU, Y. WANG, H. LIUY and K. YAO, *J. Phys. D: Appl. Phys.* **33** (2000) 2018.
4. I. YAMAGUCHI, T. MANABE, T. KUMAGAI, W. KONDO and S. MIZUTA, *Thin Solid Films* **366** (2000) 209.
5. Y. PARK, N. PARK, K. RYU, S. CHANG, S. PARK, S. YOON and D. KIM, *Bull. Korean Chem. Soc.* **22** (2001) 1015.
6. C. RAMANA, M. HUSSAIN, S. NAIDU and J. REDDY, *Thin Solid Films* **305** (1997) 219.
7. M. CHEN, H. YOU and J. GOU, *Appl. Surf. Sci.* **48–47** (1991) 12.
8. B. THI, P. MINH and B. SIMONA, *J. Appl. Phys.* **80** (1996) 7041.
9. G. ZHANG, M. MC GRAW, J. TURNER and D. GINLEY, *J. Electrochem. Soc.* **145** (1997) 163.
10. G. FANG, Z. LIU, Y. WANG, H. LIU and K. YAO, *J. Phys. D: Appl. Phys.* **33** (2000) 3018.
11. Z. LIU, G. FANG, Y. WANG, Y. BAI and K. YAO, *ibid.* **33** (2000) 2327.
12. Z. WANG, J. CHEN and X. HU, *Thin Solid Films* **375** (2000) 238.
13. I. SHIYANOVSKAYA and M. HEPEL, *J. Electrochem. Soc.* **145** (1998) 1023.
14. *Idem., ibid.* **146** (1998) 243.
15. I. SHIYANOVSKAYA, M. HEPEL and E. TEWKSBURRY, *J. New Mater. Electrochem. Syst.* **3** (2000) 241.
16. I. SHIYANOVSKAYA and M. HEPEL, *Mater. Res. Soc. Symp. Proc.* **479** (1997) 158.
17. A. TALLEDO and C. G. GRANQVIST, *J. Appl. Phys.* **77** (1995) 4655.
18. H. SHANAK, H. SCHMITT, J. NOWOCZIN and C. ZIEBERT, *Solid State Ion.* **171** (2004) 99.
19. M. KIATO, M. MAKIFUCHI and K. URABE, *Solar Energy Mater. Solar Cells* **70** (2001) 219.

20. G. WILLIAMSON and W. HALL, *Acta Metallurgica* **1** (1953) 22.
21. A. VUK, S. BENCIC, B. OREL and F. DECKER, *J. Sol-Gel Sci. Techn.* **23** (2002) 53.
22. A. TALLEDO and C. G. GRANQVIST, *J. Phys. D: Appl. Phys.* **27** (1994) 2445.
23. L. ABELLO, E. HUSSON, Y. REPELEN and G. LUCAZEAU, *J. Solid State Chem.* **56** (1985) 379.
24. M. G. KRISHNA, Y. DEBAUGE and A. K. BHATTACHARYA, *Thin Solid Films* **312** (1998) 116.

Received 9 September 2004
and accepted 18 January 2005